Dispersion Measurement in Optical Fibers Using Supercontinuum Pulses

Johan Hult, Rosalynne S. Watt, and Clemens F. Kaminski

***Abstract*—The chromatic dispersion of an optical fiber is measured using a time-of-flight technique, based on temporally and spectrally resolving a dispersed broadband pulse, on which a spectral fringe pattern has been imposed using an etalon. The technique employs broadband supercontinuum radiation, generated by launching picosecond pulses from a fiber laser into a photonic-crystal fiber. It allows the dispersion of highly dispersive optical fibers and components to be measured with a high spectral resolution over a wide wavelength region. The technique is demonstrated by measuring the dispersion of a dispersion-compensating module over its entire 400-nm transmission band with a subnanometer spectral resolution.**

***Index Terms*—Optical-fiber dispersion, optical-fiber measurements, supercontinuum radiation.**

I. Introduction

DUE TO chromatic-dispersion effects, different wavelengths propagate with different group velocities, causing short optical pulses to broaden temporally. The temporal overlapping of adjacent pulses due to chromatic dispersion thus limits the information-carrying capacity of an optical-communication system. To minimize this effect, dispersion compensation is employed; however, efficient compensation requires accurate measurements of the dispersive properties of optical fibers over a wide wavelength region. This need for broadband-dispersion measurements has been driven both by the rapid expansion of wavelength-division-multiplexing systems, which utilize a wider wavelength region, and by the need to determine higher order dispersion terms, which also requires a precise determination of the dispersion curve over a wide spectral region.

Furthermore, there are emerging applications in spectroscopy, where highly dispersive fibers are employed to transform short broadband optical pulses into rapid wavelength scans [1], [2]. To linearize the wavelength scale of such wavelength sweeps, detailed knowledge of the dispersive properties of the highly dispersive fibers employed is required.

Measurements of dispersion in optical fibers can be performed using a variety of time-of-flight, phase-shift, interferometric [3], or degenerate-four-wave-mixing-based techniques [4].

In time-of-flight methods, the time delay between either separate pulses of different wavelengths, or between different wavelength components of a single short broadband pulse, is directly detected. The resolution is limited by the shortest time delay the detector is capable of resolving. The measured time delays are then differentiated with respect to wavelength to obtain the chromatic dispersion. For this method, a pulsed light source covering a wide spectral region is required. Light sources employed include arrays of discrete-wavelength laser diodes [5] and broadband sources such as fiber Raman lasers [6], supercontinuum-radiation sources [7], [8], or tunable-soliton sources [9]. The output of such broadband sources can cover several hundred nanometers and have been spectrally filtered and scanned using a monochromator in previous studies, to achieve a reasonable spectral resolution. Supercontinuum light sources are of particular interest in this context, as they can provide broadband pulses covering extremely wide wavelength ranges [10]. The use of multiwavelength-fiber lasers that are capable of covering 30-nm wide spectral regions for time-of-flight dispersion measurements have also been reported [11].

Phase-shift methods employ an amplitude modulated, monochromatic, or spectrally filtered, continuous-wave light source. The group delay, from which the dispersion can be calculated, is determined from the phase shift between the transmitted signal and a reference signal. The wavelength of the light source needs to be scanned in order to determine the dispersion curve, which makes the measurement time consuming. In interferometric methods, the fiber to be tested forms one arm of an interferometer and a reference fiber or an air gap forms the other arm, with detection taking place in either the time or the frequency domain. From the measured cross-correlation signal, the group delay can be determined as the group delay of the reference arm is known. The drawback of such interferometric techniques is that large demands are placed on mechanical-system stability. Mapping out a dispersion curve using this method is, furthermore, time consuming, as it requires scanning of either the length of the reference arm or the wavelength of the light source employed. Supercontinuum light sources have been successfully implemented into interferometric setups for dispersion measurements over wide spectral ranges [8].

In this paper, a novel technique for accurately measuring the dispersion of highly dispersive optical fibers, based on a time-of-flight approach, is presented. It employs a pulsed supercontinuum source and an etalon, which is used to impose a spectral fringe pattern on the broadband radiation, before launching it through the fiber to be tested. By both temporally

Manuscript received July 17, 2006; revised November 8, 2006. This work was supported by Research Grant EP/C012488/1 and Advanced Research Fellowship EP/C012399/1 from the Engineering and Physical Sciences Research Council (EPSRC).

The authors are with the Department of Chemical Engineering, University of Cambridge, CB2 3RA Cambridge, U.K. (e-mail: jfh36@cheng.cam.ac.uk; rsw32@cam.ac.uk; cfk23@cam.ac.uk).

Color versions of one or more of the figures in this paper are available online at http://ieeexplore.ieee.org.

Digital Object Identifier 10.1109/JLT.2006.890422

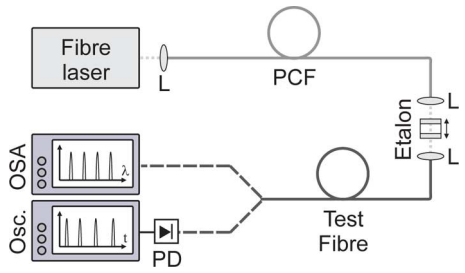

Fig. 1. Experimental setup for the supercontinuum-based fiber-dispersion measurement (L = lens, PCF = photonic-crystal fiber, PD = photo-diode, Osc = oscilloscope, OSA = optical spectrum analyzer).

and spectrally resolving the dispersed etalon fringe pattern of the pulse, the relative pulse delay can be measured, from which the dispersion can be determined. This approach allows fast measurements of the dispersion over a bandwidth of several hundred nanometers, with a spectral resolution of 1 nm or better. As the relative pulse delay is determined directly, there is no need for a calibrated reference fiber, as required by some previous techniques [6], [7]. Characterization of the dispersion using this technique is fast, as the entire dispersion curve can be determined from a single pair of temporally and spectrally resolved etalon fringe traces without the need for scanning the wavelength of the light source [9] or the detector [7]. Finally, the experimental arrangement is straightforward to implement and the instrumentation required is already available in many photonic and spectroscopic research laboratories.

II. Experimental Apparatus

A broadband pulsed supercontinuum light source was employed for the time-of-flight dispersion measurements, using the experimental setup illustrated in Fig. 1. The pump laser (FemtoPower 1060, Fianium) is a mode-locked ytterbium-fiber laser emitting pulses of 5-ps duration at a wavelength of 1065 nm. It features a built-in acoustooptic pulse-picker, which allows the repetition rate to be varied between 0.3 and 21 MHz. For the experiments presented here, a repetition rate of 1 MHz was employed to ensure that the individual pulses remain temporally separated after being dispersed through the test fiber. The supercontinuum radiation is generated in a 20-m-long photonic-crystal fiber (SC-5.0-1040, Crystal Fibre A/S), which has a zero-dispersion wavelength of 1040 nm and a mode field diameter of around 4 μm at the pump wavelength.

The output power of the supercontinuum radiation was around 18 mW when pumped by an average power of 50 mW. The spectral profile of the supercontinuum radiation generated in the photonic-crystal fiber (PCF) is shown in Fig. 2. It exhibits a relatively flat output in the spectral region stretching from 1300 to 1700 nm, which is the region of interest for characterization of the type of fibers described here. In this spectral region, the average power is around 10 μW/nm for a laser repetition rate of 1 MHz. Those average powers are sufficient for characterizing fibers featuring total losses up to 25 dB using the present detection scheme.

The supercontinuum radiation is first collimated and sent through an etalon, the purpose of which is to imprint a regular spectral pattern on the radiation. This etalon transmission

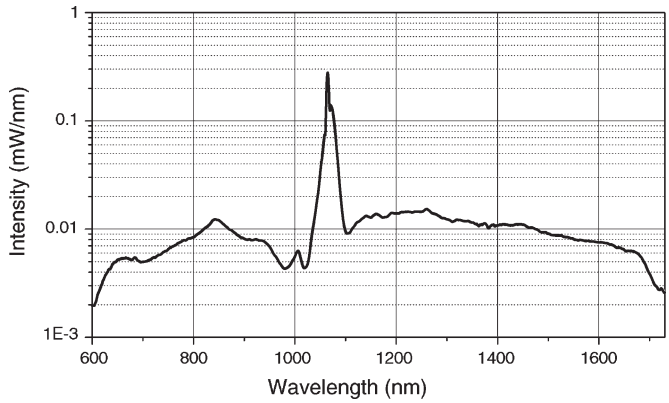

Fig. 2. Spectral profile of the supercontinuum radiation generated in the photonic-crystal fiber.

pattern will later be used to identify corresponding features of the optical pulse in both the time and wavelength domain. The home-built etalon employed is air-spaced, and the length d can be easily adjusted from about 100 μm to several millimeters, which allows for the free spectral range (FSR) to be varied according to

$$\text{FSR} = \lambda^2/2nd \tag{1}$$

where λ is the optical wavelength, and n is the index of refraction of the etalon medium—in this case air. The FSR employed determines the spectral resolution of the dispersion measurement. The broadband mirrors (PR1-1550-80-1025, CVI) employed in the etalon feature a peak reflectivity of 80% at 1550 nm resulting in a low finesse ($F < 13$). The finesse was chosen low enough to facilitate etalon alignment while still generating easily identifiable peaks over a 400-nm-wide bandwidth. A further advantage of employing a short low-finesse air-spaced etalon is that it minimizes the dispersive effect of the etalon, which is negligible compared to typical values of fiber dispersion in this paper.

The light transmitted through the etalon is then launched into the fiber to be tested. To demonstrate the technique, a dispersion-compensating module (DCM), featuring a negative dispersion of around 1.67 ns/nm at 1545 nm, was used (DC-C + L-N1650-UW, Fujikura). Both the temporal and the spectral characteristics of the dispersed optical pulse, which carries the etalon fringe pattern, are then analyzed. The spectral analysis is carried out using an optical spectrum analyzer (OSA), operating at a spectral resolution of around 0.015 nm (AQ6317C, Yokogawa). In the time domain, the dispersed pulse is resolved and recorded using a 10-GHz bandwidth-amplified photo-diode (TIA-3000, Scitec Instruments) connected to an 8-GHz bandwidth real-time oscilloscope (TDS6804B, Tektronix).

III. Results and Discussion

Dispersion measurements were carried out at both low and high spectral resolution through employing two different lengths of the etalon. The spectrally resolved etalon fringes corresponding to the shortest etalon, transmitted through the DCM and recorded by the OSA, are shown in Fig. 3(a). The individual fringes are clearly visible, and their spacing is seen

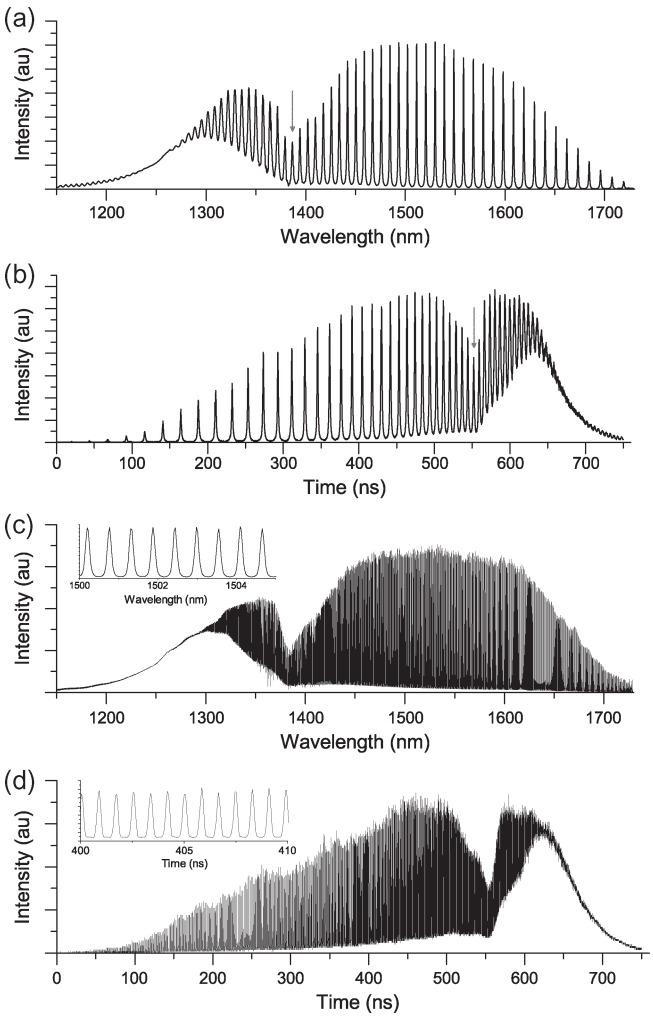

Fig. 3. Etalon fringe pattern transmitted through the test fiber. (a) and (c) Spectrally resolved using an OSA. (b) and (d) Temporally resolved using a high bandwidth photo-diode and a real-time oscilloscope. In (a) and (b), a 126-μm-long etalon was employed (FSR $=$ 9 nm at 1500 nm). In (c) and (d), a 2.03-mm-long etalon was employed (FSR $=$ 0.55 nm at 1500 nm). Insets: magnified views of the fringe patterns corresponding to the long etalon.

to increase from 6.5 nm at 1300 nm to 12 nm at 1700 nm, due to the quadratic dependence of the FSR on wavelength. The overall intensity envelope of the trace is determined by both the spectral shape of the supercontinuum radiation, shown in Fig. 2 and the DCM transmission band, shown in Fig. 4. The finesse of the etalon was observed to decrease from around 13 at 1550 nm to around 3 at 1350 nm and is seen to vanish completely below 1270 nm. The rise of the baseline below 1400 nm is due to the low finesse below this wavelength, due to reduced mirror reflectivity. From the spectral locations of the etalon fringes, the length of the etalon can be accurately determined using (1). The length of the short etalon was determined to be 126 μm using this procedure.

The same etalon fringe pattern recorded in the time domain, using the photo-diode and oscilloscope, is shown in Fig. 3(b). The longer wavelength peaks now appear to the left, as the DCM features a negative dispersion. It is clear that the difference in spacing between the longer wavelength peaks to the left and the shorter wavelength peaks to the right are larger than in

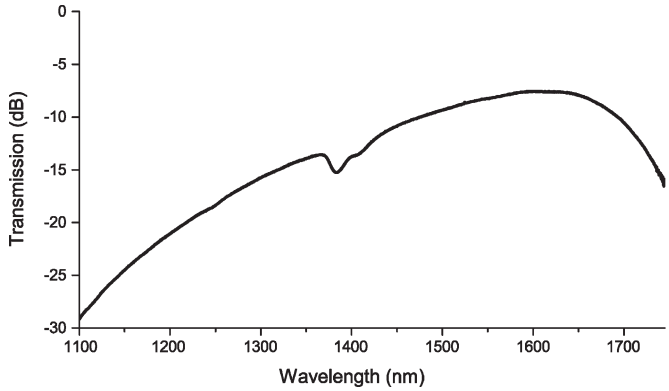

Fig. 4. Spectral transmission of the DCM.

Fig. 3(a). This indicates that the absolute value of the dispersion inside the DCM increases with wavelength. The etalon trace recorded by the oscilloscope carries a similar intensity envelope to the one recorded by the OSA but is now also affected by the spectral-response curve of the photo-diode, which decreases rapidly above 1650 nm.

To evaluate the relative pulse delay as a function of wavelength, the spectral location of each peak in the oscilloscope trace needs to be determined. First, an easily identifiable peak was used as a reference peak (marked with an arrow in Fig. 3) to establish a reference wavelength in the oscilloscope trace. In the absence of suitable spectral features in the fiber, such as the dip around 1380 nm in Fig. 4, molecular absorption lines can be used to establish a reference wavelength in the time-resolved etalon transmission trace. This is achieved, for example, by insertion of a C_2H_2 absorption cell at the position of the etalon. The wavelengths of the peaks arriving before and after the reference peak were then calculated by adding or subtracting, respectively, the relevant number of etalon FSRs from the wavelength of the reference peak. By fitting an Airy function to each individual peak, the peak center positions could be accurately determined in the time domain. In this fashion, the relative pulse delay as a function of wavelength was determined from the peak positions in the etalon trace in Fig. 3(b).

The relative pulse delay can easily be determined with higher spectral resolution by increasing the length of the etalon, resulting in a decrease of the etalon FSR. In Fig. 3(c) and (d), the etalon fringe patterns corresponding to an etalon length of 2.03 mm, recorded by the OSA and oscilloscope, respectively, are shown. For this longer etalon, the FSR varies from 0.42 nm at 1300 nm to 0.72 nm at 1700 nm, thus yielding a sub-nanometer resolution in the relative pulse-delay measurement over the entire wavelength range covered. The individual peaks, which are hardly visible in the overview traces due to the small peak spacing, are clearly resolved on both detectors as demonstrated by the magnified views shown in the insets of Fig. 3(c) and (d). In total, the fringe pattern corresponding to the long etalon comprises of 670 peaks. The identification of an isolated reference peak with a well-known wavelength on this otherwise congested oscilloscope trace was aided by the relationship between delay time and wavelength already established using the short etalon.

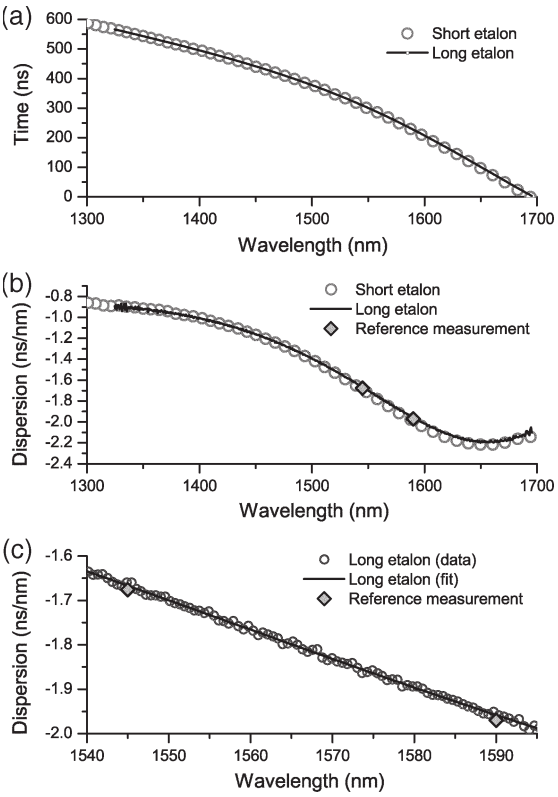

Fig. 5. (a) Relative delay of the DCM evaluated from the etalon transmission traces shown in Fig. 3. (b) Dispersion of DCM determined by direct differentiation of the relative delay data. In both figures, solid lines represent the high-resolution measurements, performed using the 2.03-mm-long etalon, and the circles represent the lower resolution measurements, performed using the 0.126-mm-long etalon. Reference values at 1545 and 1590 nm measured by the DCM manufacturer are also indicated. (c) Magnified view of the measured dispersion in the spectral region 1540–1595 nm, where circles correspond to dispersion determined directly from the relative delay data, and the solid line corresponds to dispersion determined from a polynomial fit to the relative delay data.

In Fig. 5(a), the relative pulse delays τ determined from the etalon traces, as shown in Fig. 3, are shown. From the delay, the dispersion D was calculated by direct differentiation ($D = d\tau/d\lambda$) and is shown in Fig. 5(b). From the short etalon, the dispersion could be determined over a 400-nm-wide transmission window of the DCM. The dispersion determined using the two different etalon lengths are seen to correspond well over the entire region covered, with the high-resolution measurement featuring a subnanometer resolution in the dispersion curve. Furthermore, the measured dispersion is seen to closely match independent-calibration measurements at 1545 and 1590 nm, performed by the DCM manufacturer [12]. Any initial wavelength chirp on the supercontinuum pulses before they enter the fiber to be tested will affect the accuracy of the relative time-delay measurement and, thus, the dispersion measurement. Based on the dispersion characteristics of the PCF employed for supercontinuum generation, the chirp was estimated to be smaller than 0.4 ns over the 400-nm-wide measurement interval employed here, which leads to an associated error of less than 0.1% in the measured values of dispersion.

The high resolution in the dispersion data is demonstrated in Fig. 5(c), which shows the dispersion in a short interval around 1570 nm. The dispersion evaluated through direct differentiation of the delay is shown as circles, whereas the straight line corresponds to dispersion evaluated through differentiation of a polynomial fit to the delay data. The root-mean-square of the difference between the two dispersion curves shown in Fig. 5(c) is only 0.6%, which confirms the small scatter in the directly determined dispersion values. As only two spectra—one recorded using an OSA and one recorded using an oscilloscope—are required to calculate the dispersion over the entire bandwidth the measurement procedure allows for very fast dispersion measurements.

IV. Conclusion

In this paper, we have presented the application of a broadband supercontinuum light source for measuring the dispersion curve in high-dispersion fibers by a time-of-flight technique. By employing an etalon to impose a spectral fringe pattern on the broadband pulse, the dispersion can be measured with a high spectral resolution (< 1 nm) over a several-hundred-nanometer-wide spectral region. The technique is simple to implement, as supercontinuum light sources are becoming increasingly common in research laboratories, and as standard spectrum analyzers, photo-diodes and oscilloscopes can be employed for detection.

The dispersion-measurement technique presented here cannot directly be implemented to characterize fibers, where the zero-dispersion wavelength falls within the measurement range, as multiple etalon peaks around this wavelength would arrive at the same time at the detector. However, by inserting the fiber to be tested after a previously characterized high-dispersion fiber (e.g., the DCM employed in this paper), measurements of dispersion should also be possible in fibers featuring a zero-dispersion wavelength, albeit at slightly reduced accuracy. In such a scheme, care must be taken to ensure that the sign and magnitude of the dispersion of the high-dispersion fiber employed is chosen such that a high absolute value of dispersion of the two combined fibers is maintained.

By improving the temporal resolution in the detection, through the use of a higher bandwidth photo-diode and a sampling oscilloscope, in combination with an increased length of the etalon, the technique could be extended to measure smaller values of dispersion or to provide higher spectral resolution in the dispersion measurement. However, the time-bandwidth product of the observed etalon peaks sets a fundamental limit to the maximum spectral resolution attainable: As the etalon is made longer, the peak spacing will decrease, thus increasing the spectral resolution of the measurements. The associated spectral narrowing of the etalon peaks initially leads to a corresponding narrowing of the peaks in the time domain. At some point, however, the time-bandwidth product will limit further decreases in the temporal width of the peaks. This will lead to a gradual decrease in finesse in the time-resolved etalon transmission trace. This apparent decrease in finesse will eventually compromise the accuracy of the relative time-delay measurement. In this paper, this effect imposes a limit on the highest spectral resolution in the dispersion measurements of about 0.1 nm.

REFERENCES

[1] P. V. Kelkar, F. Coppinger, A. S. Bhushan, and B. Jalali, "Time-domain optical sensing," *Electron. Lett.*, vol. 35, no. 19, pp. 1661–1662, Sep. 1999.

[2] S. T. Sanders, "Wavelength agile fibre laser using group-velocity dispersion of pulsed supercontinua and application to broadband absorption spectroscopy," *Appl. Phys. B, Photophys. Laser Chem.*, vol. 75, no. 6/7, pp. 799–802, Nov. 2002.

[3] L. G. Cohen, "Comparison of single-mode fiber dispersion measurement techniques," *J. Lightw. Technol.*, vol. LT-3, no. 5, pp. 958–966, Oct. 1985.

[4] L. F. Mollenauer, P. V. Mamyshev, and M. J. Neubelt, "Method for facile and accurate measurements of optical fiber dispersion maps," *Opt. Lett.*, vol. 21, no. 21, pp. 1724–1726, Nov. 1996.

[5] C. Lin, A. R. Tynes, A. Tomita, P. L. Liu, and D. L. Philen, "Chromatic dispersion measurements in single-mode fibers using picosecond InGaAsP injection lasers in the 1.2- to 1.5-μm spectral region," *Bell Syst. Tech. J.*, vol. 62, no. 2, pp. 457–462, Feb. 1983.

[6] L. G. Cohen and C. Lin, "A universal fiber-optic (UFO) measurement system based on a near-IR fiber Raman laser," *IEEE J. Quantum Electron.*, vol. QE-14, no. 11, pp. 855–859, Nov. 1978.

[7] K. Mori, T. Morioka, and M. Saruwatari, "Group velocity dispersion measurement using supercontinuum picosecond pulses generated in an optical fibre," *Electron. Lett.*, vol. 29, no. 11, pp. 987–989, May 1993.

[8] F. Koch, S. V. Chernikov, and J. R. Taylor, "Dispersion measurement in optical fibres over the entire spectral range from 1.1 μm to 1.7 μm," *Opt. Commun.*, vol. 175, no. 1–3, pp. 209–213, Feb. 2000.

[9] N. Nishizawa, A. Muto, and T. Goto, "Measurement of chromatic dispersion of optical fibers using wavelength-tunable soliton pulses," *Jpn. J. Appl. Phys.*, vol. 39, no. 8, pp. 4990–4992, Aug. 2000.

[10] R. R. Alfano, *The Supercontinuum Laser Source*, 2nd ed. New York: Springer-Verlag, 2006.

[11] J.-N. Maran, R. Slavík, S. LaRochelle, and M. Karásek, "Chromatic dispersion measurement using a multiwavelength frequency-shifted feedback fiber laser," *IEEE Trans. Instrum. Meas.*, vol. 53, no. 1, pp. 67–71, Feb. 2004.

[12] K. Mezaki, private communication, Sakura, Japan: Fujikura Ltd., Apr. 2006.

Johan Hult received the M.Sc. and Ph.D. degrees in engineering physics from Lund University, Lund, Sweden, in 1998 and 2002, respectively.

He is currently an EPSRC Advanced Research Fellow with the Department of Chemical Engineering, University of Cambridge, Cambridge, U.K., which he joined as a Marie Curie Research Fellow in 2002. He is also the holder of a Senior Research Fellowship of Magdalene College, Cambridge. His research interests focus on atomic and molecular laser spectroscopy, reactive-flow diagnostics, and the development of novel laser-based sensors and laser sources.

Rosalynne S. Watt received the B.Sc. degree (with honors) in mathematics and physics from the University of Glasgow, Glasgow, U.K., in 2003 and the M.Sc. degree in optics and photonics from the Imperial College of Science and Technology, London, U.K., in 2004. She is currently working toward the Ph.D. degree at the Department of Chemical Engineering, University of Cambridge, U.K., which she joined in 2005.

Her research focuses on the development of a supercontinuum laser source for gas sensing in combustion and reactive-flow systems.

Clemens F. Kaminski received the B.Sc. degree in physics and electronics from the University of Reading, Reading, U.K., in 1991 and the D.Phil. degree in physics from the University of Oxford, Oxford, U.K., in 1995.

From 1995 to 2000, he was a Marie Curie Research Fellow and, later, an Associate Professor in engineering physics at Lund University, Lund, Sweden. He is currently a Reader with the Department of Chemical Engineering, University of Cambridge, Cambridge, U.K., which he joined as a Lecturer in 2001. He is also a Fellow of Robinson College, Cambridge. He heads the Laser Analytics Group, which is active within the fields of reactive-flow imaging, sensor design, and micro and nanoscale diagnostics. His particular research interest are in the development and application of fluorescence-based imaging techniques for the study of chemistry and in systems ranging from living cells to gas-turbine combustors.